

# Asymmetric Linker Histone Association Directs the Asymmetric Rearrangement of Core Histone Interactions in a Positioned Nucleosome Containing a Thyroid Hormone Response Element<sup>†</sup>

Dmitry Guschin, Simon Chandler, and Alan P. Wolffe\*

Laboratory of Molecular Embryology, National Institute of Child Health and Human Development, National Institutes of Health, Building 18T, Room 106, Bethesda, Maryland 20892-5431

Received March 16, 1998; Revised Manuscript Received April 16, 1998

**ABSTRACT:** We describe histone–DNA cross-linking in a positioned nucleosome containing a thyroid hormone response element (TRE) from the *Xenopus laevis* thyroid hormone receptor  $\beta$ A gene (TR $\beta$ A). Histones H3 and H4 are cross-linked to DNA in the nucleosome core within 30 base pairs to either side of the dyad axis. Histone H2A cross-links to DNA in the core at the dyad axis, and histones H2A and H2B have extensive interactions with DNA 40–80 bp away from the dyad axis. Linker histone H5 and the globular domain of *Xenopus* H1<sup>o</sup> associate asymmetrically with DNA at one edge of the TR $\beta$ A nucleosome. Nevertheless, the asymmetric association of H5 leads to a significant rearrangement of core histone–DNA contacts at the dyad axis of the nucleosome. In the presence of linker histone, cross-linkings of H4 within 15 bp to one side of the dyad axis, of histone H2A at the dyad axis, and of H2A and H2B 40–80 bp to one side of the dyad axis are all reduced. This reduction in cross-linking occurs preferentially on the side of the nucleosome to which H5 is bound. Our results indicate that core histone contacts within mononucleosomes are conformationally dynamic and that linker histone incorporation at the edge of the nucleosome can influence core histone–DNA interactions in an asymmetric way including contacts at the dyad axis.

Nucleosomal architecture and histone modification have essential roles in gene regulation (1–4). Histone acetylation is required for the activation of specific genes in vivo (5), and linker histones can activate or repress specific genes in vivo (6–8). Interpretation of these effects requires detailed information concerning the structural roles of the individual histones and their domains with respect to DNA sequences within the nucleosome. Crystallographic analysis reveals the extensive intermolecular contacts made by the core histones between themselves (9–11) and with DNA (12). Despite this progress, the exact positions of the core histone amino termini and the binding site for linker histone in the nucleosome appear to be variable (12–17).

A powerful tool in the analysis of histone–DNA interactions in nucleosomes and chromatin is DNA–protein cross-linking (18–23). These studies have established that rearrangement of core histone–DNA contacts can occur during the disassembly of chromatin isolated from endogenous chromosomes dependent on the removal of either linker histones or linker DNA (24, 25). In contrast, our experiments have focused on the *reconstruction* of histone–DNA interactions in chromatin using purified histones and DNA sequences that position nucleosomes (reviewed in ref 26). We have used chemical footprinting to orientate the double helix

on the surface of the core histones (27) and protein–DNA cross-linking to map histone–DNA contacts (13, 28). In contrast to prevailing models of linker histone association with nucleosomes containing a mixture of DNA sequences (29–31), we find an asymmetric association of linker histone with a nucleosome containing a *Xenopus borealis* somatic 5S rRNA gene (13, 14, 28, 32). To test whether the association of linker histone with the 5S nucleosome is an exceptional circumstance or might be a more general phenomenon, we have extended our analysis to another positioned nucleosome containing a unique DNA sequence from the *Xenopus laevis* thyroid hormone receptor  $\beta$ A gene (TR $\beta$ A). Chromatin assembly and modification have significant roles in the transcriptional control of the *Xenopus* TR $\beta$ A gene in vivo (33–36).

We find that a DNA fragment from the TR $\beta$ A gene that contains the thyroid hormone response element (TRE) is assembled into a positioned nucleosome core. Within this nucleosome core the double helix is rotationally positioned with respect to the surface of the core histones and the core histones are translationally positioned such that DNA–histone contacts begin and end at a particular sequence. Inclusion of linker histones into the nucleosome occurs asymmetrically at one edge of the nucleosome core. Incorporation of the linker histone results in an asymmetric rearrangement of core histone contacts including those at the dyad axis. Such a conformational change in the nucleosome might contribute to observed alterations in the path of DNA within the nucleosome that occur as a

<sup>†</sup> S.C. is the recipient of a Wellcome Trust Prize International Fellowship.

\* To whom correspondence should be addressed (phone 301-402-2722; Fax 301-402-1323; E-mail awlme@helix.nih.gov).

consequence of linker histone binding.

## MATERIALS AND METHODS

**Reconstitution.** The 176 bp *AccI*–*DdeI* DNA fragment containing the *X. laevis* TR $\beta$ A gene (from +156 to +332 relative to the start site of transcription at +1) was radiolabeled at a single restriction site using polynucleotide kinase and [ $\gamma$ -<sup>32</sup>P]ATP for protein–DNA cross-linking, linker histone binding, and hydroxyl radical cleavage analysis. The same DNA fragment was left unlabeled for mapping of the translational position of the histone octamer. Nucleosome cores were reconstituted onto DNA fragments by exchange from chicken erythrocyte core particles (37). In the histone exchange method, a 15-fold template mass excess of core particles was mixed with radiolabeled DNA in tubes followed by slow adjustment of NaCl concentration (to 1 M). Tubes were incubated at 37 °C for 15 min. Samples were transferred to a dialysis bag (with a molecular size limit of 6–8 kDa) and dialyzed against 1.0 M NaCl, 10 mM Tris-HCl, pH 7.5, 1 mM EDTA, and 0.1 mM phenylmethanesulfonyl fluoride (PMSF) for 4 h at 4 °C and then dialyzed in 0.75 M NaCl buffer for 4 h, followed by a final dialysis overnight against 10 mM Tris-HCl, pH 7.5, and 0.1 mM EDTA.

**Linker Histone Binding Experiments.** A total of 100 ng (DNA content) of nucleosome cores (0.6 pmol) was incubated with various amounts of linker histone as indicated in 10  $\mu$ L of binding buffer [10 mM HEPES–NaOH, pH 7.4/50 mM NaCl/0.1 mM EDTA/5% (v/v) glycerol] at room temperature for 15–30 min (32). Samples were analyzed by 6% PAGE in 0.5  $\times$  TBE. After electrophoresis, the gels were dried and autoradiographed.

**Micrococcal Nuclease Mapping of Translational Positioning.** Mononucleosomes (80 ng of DNA) (molar ratio of histone to DNA = 1) were digested with 0.075–0.6 unit of micrococcal nuclease (Pharmacia) for 5 min at 22 °C. Incubation with linker histone was as described above. Ca<sup>2+</sup> was adjusted to 0.5 mM concomitantly with addition of micrococcal nuclease. Digestions were terminated with addition of EDTA (5 mM), SDS (0.25%, wt/v), and proteinase K (Gibco-BRL) (1 mg/mL). The DNA was recovered and 5'-end-labeled with [ $\gamma$ -<sup>32</sup>P]ATP and T4 polynucleotide kinase, and the end-labeled DNA fragments were separated by electrophoresis in nondenaturing 6% polyacrylamide gels. DNA fragments of nucleosome core and chromatosome products were recovered and digested with restriction endonucleases to determine micrococcal nuclease cleavage sites (32). Digestions were incomplete at the concentrations of restriction endonuclease used; hence, some 146 and 161 bp length DNAs remain in the digests.

**DNase I and Hydroxyl Radical Footprinting of Rotational Positioning.** Reconstitutes with or without linker histone were treated with either DNase I or hydroxyl radicals before nucleoprotein complexes were resolved on 6% PAGE (38). Samples containing labeled mononucleosomes (60 ng of DNA) were incubated with or without linker histone as described; the exact amount corresponding to one molecule per nucleosome core was determined by gel shift. Naked DNA was digested with 12 ng of DNase I (Gibco-BRL); nucleosome cores without linker histone and nucleosome cores with linker histone were digested with 30–60 ng of

enzyme. DNase I reactions were carried out at room temperature for 1 min and terminated by addition of EDTA (5 mM). Glycerol (5% v/v) was added to the sample, and the entire reaction volume was transferred directly into a preparative gel. The hydroxyl radical cleavage reactions were carried out as described (27). Free radical reactions were quenched with the addition of glycerol to a concentration of 5%, and the entire volume was applied to a gel, as described above. After electrophoresis, linker histone bound or unbound nucleosome complexes were excised from gel. DNA from these complexes was isolated and analyzed by denaturing polyacrylamide (6%) gel electrophoresis. Specific DNA makers were produced by Maxam and Gilbert cleavage at G residues.

**DNA–Protein Cross-Linking.** In these experiments chemical cross-linking of histones to DNA is performed using DNA within the nucleosome core particles that has been end-labeled with <sup>32</sup>P so that the position of histone–DNA contacts relative to the end of the molecule (as a reference point) can be determined. This is followed by reaction with dimethyl sulfate, which methylates purine bases. The methylated product is then depurinated to an aldehyde. A Schiff base is formed between the modified DNA backbone and available lysine or histidine amino acids in the histones, which can be further stabilized by reduction with sodium borohydride (17, 39). Very low levels of reaction are allowed so that a wide distribution of DNA–histone cross-links are generated. Exact reaction conditions are given below.

Methylation of DNA within the nucleoprotein complex was as described (39). This employed 10–25 mM dimethyl sulfate followed by incubation in 15 mM HEPES–NaOH, 50 mM NaCl, 0.1 mM PMSF, pH 7.4, and 0.1 mM EDTA, at 37 °C (resulting in partial depurination and subsequent cross-linking). The reaction was stopped by the addition of 25 mM NaBH<sub>4</sub> in 50 mM HEPES–NaOH, pH 7.4 on ice, followed by dialysis into 15 mM HEPES–NaOH, pH 7.4, 50 mM NaCl, and 0.1 mM EDTA. We have previously shown that the 5S nucleosome core under these conditions is stable to protracted heating at temperatures as high as 55 °C (40). Nucleosome mobility on nondenaturing gels is dependent on the translational positioning of the histone octamer relative to the DNA fragment (41). The cross-linking procedure itself (DMS treatment and borohydride reduction steps) does not alter the mobility of the TR $\beta$ A nucleosome core (not shown).

**Purification of Cross-Linked Products.** DNA with covalently attached proteins was ethanol precipitated in the presence of 0.5% SDS. The reaction was supplemented with 0.5 mg/mL unlabeled mixed-sequence nucleosome cores isolated from chicken erythrocytes as a carrier. The protein-tagged DNA fragments were purified by KCl–SDS precipitation as described (39) and dissolved in loading buffer containing 9 M urea.

Two-dimensional electrophoresis was done as described (39). For the electrophoresis leading to the gels and autoradiograms shown in this work, the first dimension requires the resolution of histone–DNA adducts, and the second dimension requires the resolution of different DNA fragments, as described below. The first dimension (from left to right in the autoradiograms) requires denaturation of the histone–DNA complex by boiling in 1% SDS and 7 M

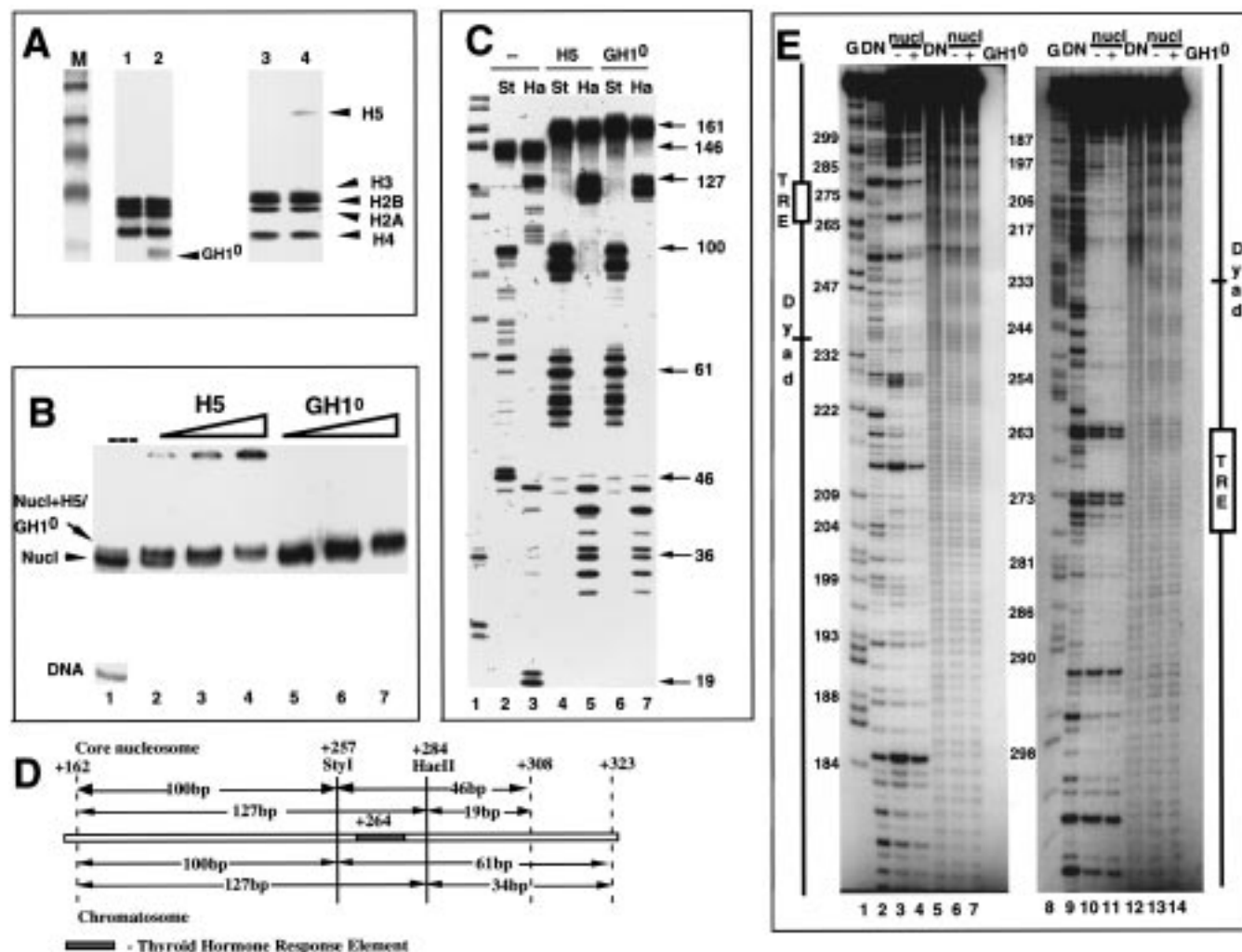


FIGURE 1: (A) SDS-PAGE showing histone composition of nucleosomes containing the TR $\beta$ A gene (TRE nucleosome). Lanes: 1, nucleosome core; 2, nucleosome with globular domain of H1° linker histone; 3, nucleosome core; 4, nucleosome with the H5 linker histone. (B) Characterization of linker histone binding to nucleosomes containing the TR $\beta$ A gene. Lanes: 1, TRE nucleosome core; 2–4, TRE nucleosome with increasing amounts of histone H5 (1-, 2-, and 4-fold molar ratio, respectively); 5–7, TRE nucleosome with increasing amounts of globular domain of the linker histone H1° (1-, 2-, and 4-fold molar ratio, respectively). (C) Asymmetric protection of linker DNA from micrococcal nuclease in TRE nucleosome. Lane 1 shows markers. Lanes 2 and 3 show nucleosome core DNA (146 bp) cut with *StyI* and *HaeII*, respectively. Lanes 4 and 5 show chromatosome DNA (161 bp) from H5 containing nucleosomes cut with *StyI* and *HaeII*, respectively. Lanes 6 and 7 show chromatosome DNA (161 bp) from GH1° containing nucleosomes cut with *StyI* and *HaeII*, respectively. (D) Schematic representation of micrococcal nuclease mapping data (Figure 1C). Locations of fragments from the *StyI* and *HaeII* mapping experiment of the nucleosome core and chromatosome DNA are shown with respect to the TRE element (gray box). (E) Rotational positioning of DNA in the TRE nucleosome is not changed by GH1° linker histone association. Lanes 1–7 show mapping on the top strand. Lanes: 1, G-specific cleavage reaction; 2–4, DNase I mapping of (lane 2) naked DNA, (lane 3) nucleosome core, and (lane 4) nucleosome with GH1°; 5–7, hydroxyl radical mapping of (lane 5) naked DNA, (lane 6) nucleosome core, and (lane 7) nucleosome with GH1°. Lanes 8–14 show mapping on the bottom strand. Lanes: 8, G-specific cleavage reaction; 9–11, DNase I mapping of (lane 9) naked DNA, (lane 10) nucleosome core, and (lane 11) nucleosome with GH1°; 12–14, hydroxyl radical mapping of (lane 12) naked DNA, (lane 13) nucleosome core, and (lane 14) nucleosome with GH1°.

urea and resolution of histone–DNA adducts on a 15% acrylamide gel containing 0.15% SDS and 7 M urea. The mobility of the DNA molecule is reduced by the cross-linked protein. Resolution in a second dimension (from top to bottom in the autoradiograms) follows removal of the histones from DNA with a protease; this allows sizing of the DNA fragments. The second dimension again uses a 15% acrylamide gel containing 0.1% SDS and 7 M urea. The relative mobility of protein-bound and free DNA permits the organization of the histones relative to the end of DNA in the nucleosomal core particle to be determined.

Assignment of spots of cross-linked DNA fragments to individual histones was based upon comparison with the positions of G+A cleavage products in the gel.

## RESULTS AND DISCUSSION

### Nucleosome Reconstitution on the TR $\beta$ A Gene Fragment.

In earlier work we have reconstituted nucleosomes onto PCR-generated 204 bp long DNA fragments from +159 to +363 relative to the start site of transcription at +1 (35). This 204 bp fragment was found to be rotationally positioned relative to the surface of the histone octamer but showed multiple translational positions of the histone octamer with respect to the DNA sequence. Because shorter DNA fragments reduce variation in translational positioning (see refs 32 and 42), we chose to use a shorter fragment of 176 bp from +156 to +332 relative to the start of transcription

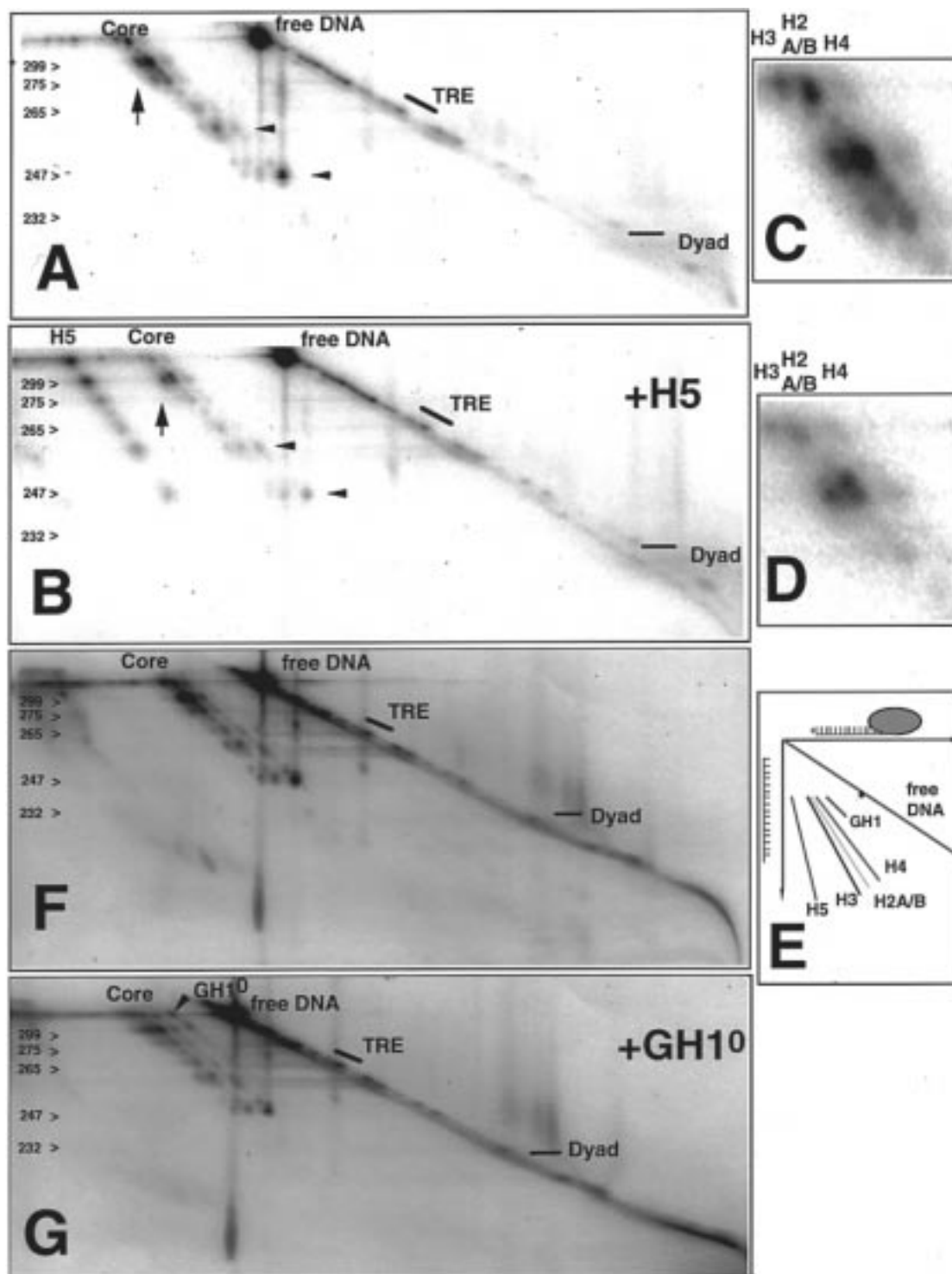


FIGURE 2: Mapping of histone DNA contacts with the top strand of the nucleosomes containing the TR $\beta$ A gene in the absence (A) or presence (B) of the H5 linker histone. Vertical arrows indicate sites of major rearrangement in core histone–DNA contacts at the periphery of the nucleosome. Horizontal arrowheads indicate H4 contacts around the dyad axis. (C and D) Enlargement of the area indicated by an arrow in panels A and B. (E) Scheme of 2D gel electrophoresis. Mapping of histone–DNA contacts with the top strand of the nucleosomes containing the TR $\beta$ A gene in the absence (F) or presence (G) of the globular domain of linker histone H1 $^{\circ}$  (GH1 $^{\circ}$ ).

at +1 flanked by *AccI* and *DdeI* restriction sites. We prepared nucleosome cores by histone exchange and monitored the histones reconstituted into nucleosomes by gel electrophoresis (Figure 1A) and nucleosome reconstitution itself by gel shift (Figure 1B, lane 1). Addition of either chicken erythrocyte H5 (lanes 2–4) or the recombinant winged helix globular domain of H1 $^{\circ}$  (GH1 $^{\circ}$ , lanes 5–7) leads to the retardation of the nucleosome core, suggesting

stable incorporation of linker histone into the nucleosome. Micrococcal nuclease digestion revealed that a kinetic intermediate in digestion of 161 bp in length (Figure 1C, 161 bp) was generated on the inclusion of linker histones into the TR $\beta$ A nucleosome. In contrast, only 146 bp of DNA were protected by the core histone octamer alone (Figure 1C, 146 bp). End-labeling of the 161 and 146 bp fragments followed by restriction endonuclease digestion allowed us

to map the boundaries of the stable histone–DNA interaction in the absence and presence of linker histone (Figure 1C,D). In the absence of linker histone, the core histones protect 146 bp of DNA with a 5' boundary at +162 and a 3' boundary at +308. Inclusion of either histone H5 or GH1° protects an additional 15 bp of linker DNA from digestion (Figure 1C). Comparison of DNA fragment sizes shows that the 5' boundary of histone–DNA protection remains the same at +162 but that the 3' boundary is extended 15 bp to +323. This asymmetric protection of linker DNA from +308 to +323 to one side of the nucleosome core is similar to that obtained when linker histones are reconstituted into nucleosomes containing the *X. borealis* somatic 5S rRNA gene (32, 42). The incorporation of linker histone is without effect on the rotational or translational positioning of the TR $\beta$ A DNA on the surface of the histone octamer (Figure 1E; see Figures 2–4 later). Our next experiments examine the histone–DNA contacts in the TR $\beta$ A nucleosome in the presence or absence of linker histone.

**Histone–DNA Contacts in the TR $\beta$ A Nucleosome Core.** In the absence of linker histone, the micrococcal nuclease digestion data (Figure 1) indicate that the histone octamer adopts a single dominant translational position on the TR $\beta$ A gene with the dyad axis centered at +234 (relative to the start of transcription at +1). In the nucleosome the minor groove of the double helix will face away from the histone octamer at the dyad axis and toward the octamer 0.5 and 1.5 turns to either side of the dyad axis (43). In the TR $\beta$ A nucleosome, the minor groove faces toward the histone octamer at +237 and +247 with respect to the bottom strand and at +240 and +250 for the top strand (Figure 1E). Important features of nucleosome core structure determined from the crystal structure (12) and from cross-linking studies (20, 23, 44) are two sites of strong cross-linking between histone H4 and DNA at a distance of 1.5 helical turns to either side of the dyad axis. At this point the major groove faces out toward solution where the N-terminal  $\alpha$ -helices of the H3–H4 heterodimers cause DNA to be maximally bent with the double helix having an outward bulge (12). Within the TR $\beta$ A nucleosome core, histone H4 cross-linking is detected to either side of the dyad axis between +211 and +261 with the major sites located at +247 and +261 for the top strand (Figure 2A, arrowheads) and at +219, +244, and +258 for the bottom strand (Figure 3A). The N-terminal tail of histone H4 associates with DNA at multiple sites (44). A second feature of histone–DNA interactions around the dyad axis is the presence of the C-terminal tail of histone H2A in contact with DNA (12, 45, 46). Within the TR $\beta$ A nucleosome strong histone H2A cross-linking is detected at the dyad axis around +234 (Figure 3A, open arrowhead). Extensive cross-linking of histones H2A/H2B are also detected from 40 to 80 bp to either side of the nucleosomal dyad (Figures 2A and 3A). The N-terminal tail of histone H2A is known to associate with DNA at multiple sites (16). We conclude that the core histone–DNA contacts detected within the TR $\beta$ A nucleosome core are consistent with our mapping of the nucleosome core dyad to +234 (see Figure 4).

**Inclusion of Linker Histones H5 Leads to an Asymmetric Rearrangement of Core Histone–DNA Contacts in the Nucleosome.** The incorporation of intact linker histone H5 into the TR $\beta$ A nucleosome (Figure 1B) is associated with

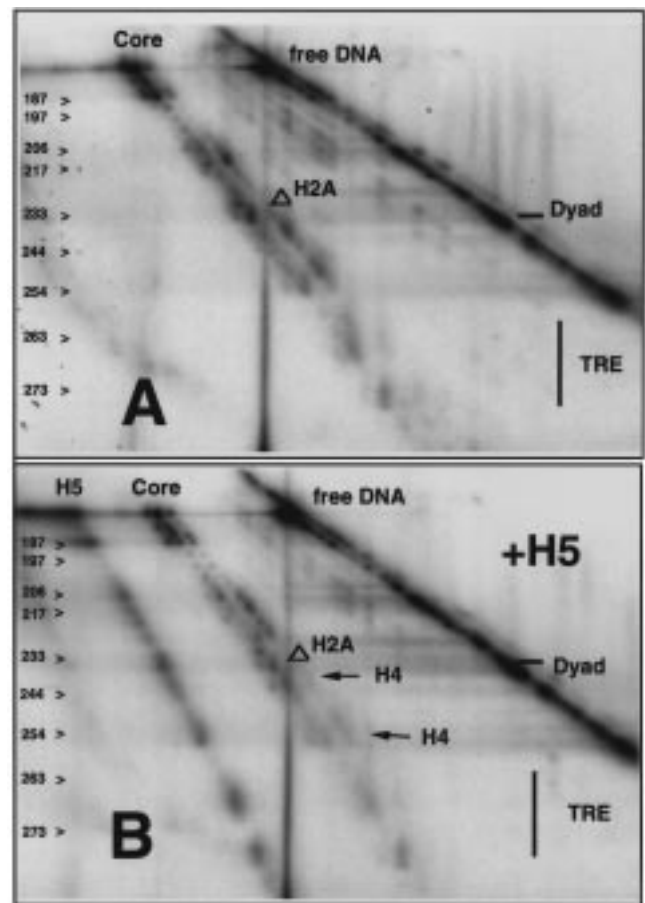


FIGURE 3: Mapping of histone–DNA contacts with the bottom strand of nucleosomes containing the TR $\beta$ A gene in the (A) absence or (B) presence of H5 linker histone. The open arrowhead indicates the site of H2A cross-linking around the dyad axis. Arrows in (B) indicate H4 contacts that are reduced on inclusion of H5 into the nucleosome.

the appearance of numerous new cross-linking contacts made by this histone with DNA (Figure 2B and Figure 3B, H5). These are distributed throughout nucleosomal DNA as previously observed for the *X. borealis* 5S nucleosome (13). Remarkably, incorporation of H5 leads to an asymmetric loss of H4–DNA contacts to one side of the dyad axis between +247 and +261 (Figure 3, compare panels A and B, arrows marked H4). Contacts made by H4 with DNA between +207 and +222 remain intact in the presence of H5. There is also a loss of H2A cross-linking at the dyad axis (+232) as a consequence of linker histone incorporation (Figure 3B, open arrowhead). Core histone contacts of H2A and H2B at the periphery of the nucleosome from +275 to +323 are significantly reduced on incorporation of histone H5 (Figure 2A,B vertical arrow, and 2C,D). These sites are proximal to the linker DNA protected by H5 from micrococcal nuclease digestion and where sites of strong H5–DNA cross-linking are detected (Figure 1C,D; see Figure 4). Thus, the incorporation of histone H5 into the nucleosome leads to a selective reduction in the efficiency of cross-linking of core histones to nucleosomal DNA. The core histone–DNA contacts on the side of the nucleosome away from the protected linker DNA are largely unaffected by inclusion of the linker histone (Figure 3A,B). In contrast, on the side of the nucleosome proximal to where the linker histone binds, both H4 and H2A/H2B contacts are reduced (Figure 2A,B,

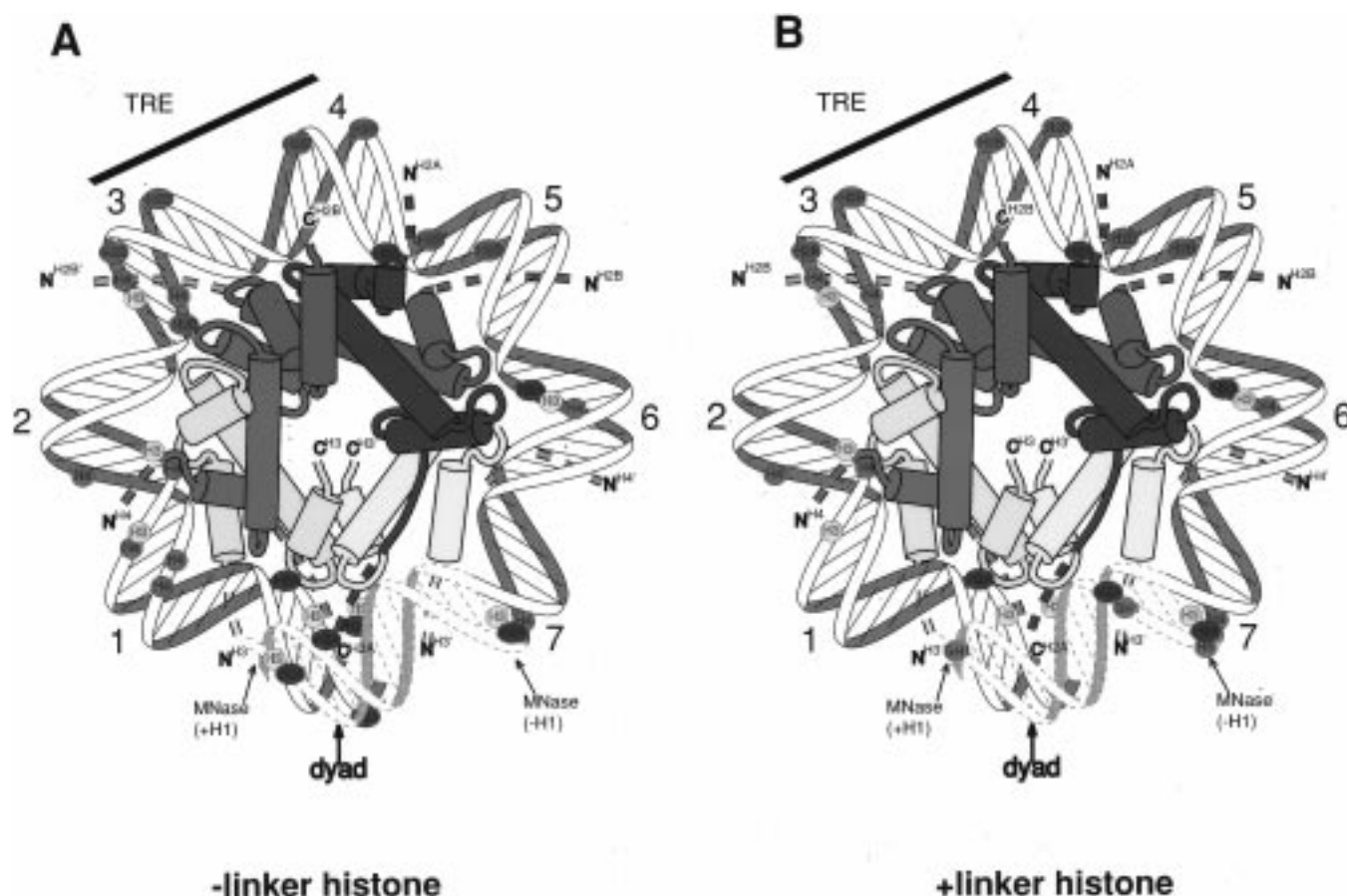


FIGURE 4: Architecture of histone-DNA contacts in the nucleosome containing the TR $\beta$ A gene with and without linker histone. The micrococcal nuclease protection boundaries and sites of histone-DNA contacts are shown. For simplicity, the DNA is presented as a uniform superhelix. Histone H4 is shown in red, H3 in yellow, H2B in blue, and H2A in green. The positions of the dyad axis and the TRE are indicated.

arrows, Figure 2C,D, Figure 3A,B).

*Inclusion of GH1° Reveals an Asymmetric Association with the TR $\beta$ A Nucleosome Core but Does Not Rearrange Core Histone DNA Contacts at the Dyad Axis.* In earlier work using the *X. borealis* somatic 5S rRNA gene we have detected a much more localized association of the globular winged helix domain of H5 with nucleosomal DNA as opposed to the generalized binding of the intact protein (13). Incorporation of GH1° into the TR $\beta$ A nucleosome core does not lead to significant alteration in core histone interactions with DNA at the nucleosomal dyad (Figure 2E–G). Cross-linking of GH1° to DNA in these experiments is detected at +311 and +323 (Figure 2G). These cross-linking contacts are consistent with the protection of linker DNA (or more correctly extranucleosomal DNA as there is no second nucleosome) from micrococcal nuclease digestion (Figure 1C,D). There is also some loss of core histone cross-linking between +295 and +323 (Figure 2C,D). We suggest that the globular winged helix domain of the linker histone can be assembled into the TR $\beta$ A nucleosome at a highly asymmetric position. However, the incorporation of the globular domain alone does not lead to major alterations in core histone-DNA contacts in the TR $\beta$ A nucleosome. In contrast, incorporation of the intact histone H5 does lead to rearrangements albeit in a highly asymmetric manner (Figures 2 and 3). Thus, we suggest that the N- and C-terminal tails of the linker histone that flank the globular domain interact with DNA as it wraps around the histone octamer

and are competing with the core histone N- and C-terminal tails for contacts. These interactions preferentially occur on the side of the nucleosome proximal to the binding site for the globular domain of H5. It should be noted that most of the histone-DNA contacts detected using the cross-linking approach employed in this paper are made by the tail domains (46, 47).

## CONCLUSIONS

We conclude that the globular domain of a linker histone (H1°) has a highly asymmetric interaction with a nucleosome core including the TR $\beta$ A gene. Association of the globular domain alone leads to very little rearrangement of core histone-DNA contacts in the nucleosome core. However, if an intact linker histone H5 is used for reconstitution, then additional contacts are made by the linker histone with DNA in the nucleosome and core histone contacts are rearranged (summarized in Figure 4). We suggest that the asymmetric association of a linker histone at the edge of a nucleosome mediated by the globular domain can lead to a dynamic reconfiguration of core histone-DNA interaction including those at the dyad axis. Such a rearrangement at the dyad axis might contribute to alterations in the path or cleavage of DNA at the dyad axis as a consequence of linker histone association (31, 48, 49). The rearrangement of core histone contacts also has a significant asymmetric component. This provides additional support for the existence of asymmetric

nucleosomes, an arrangement that might be propagated in vivo (50).

Several recent papers are consistent with our proposal of an asymmetric association of linker histones with the nucleosome core (26, 32). The winged helix transcription factor HNF3 that is isomorphous with the globular domain of linker histones binds to nucleosomal DNA asymmetrically (51). Site-directed mutants of HNF3 can compact nucleosomal DNA if they contain basic amino acids at sites previously shown to be important for nucleosomal DNA compaction by linker histones (51, but see ref 52). Several other nucleosomes assembled on defined DNA sequences also show asymmetric protection of linker DNA to micrococcal nuclease digestion (35, 53, 54). It should be noted that micrococcal nuclease digestion alone provides only circumstantial evidence for asymmetric (or symmetric) linker histone association due to potential sequence preferences in sites of cleavage. Hence, careful control of enzyme concentrations during digestion and additional methodologies such as protein–DNA cross-linking or novel DNA cleavage reagents need to be used (13, 14, 28, this work). Our results with the TR $\beta$ A nucleosome are significant in this regard because both the *Lytechinus variegatus* and *X. borealis* 5S rRNA genes used for many nucleosome positioning studies have very similar sequences and are identical in the linker DNA region protected by linker histones on the *X. borealis* gene from micrococcal nuclease digestion (55, 56). Future studies must explore whether the asymmetric model of the nucleosome holds for higher order chromatin structures beyond the dinucleosome (42).

## ACKNOWLEDGMENT

We thank Dr. Jeffrey Hayes for the kind gift of recombinant H10, D. Pruss for original art, and Ms. Thuy Vo for manuscript preparation.

## REFERENCES

1. Paranjape, S. M., Kamakaka, R. T., and Kadonaga, J. T. (1994) *Annu. Rev. Biochem.* 63, 265–297.
2. Wallrath, L. L., Lu, Q., Granok, H., and Elgin, S. C. R. (1994) *BioEssays* 16, 165–170.
3. Brownell, J. E., Zhou, J., Ranalli, T., Kobayashi, R., Edmondson, D. G., Roth, S. Y., and Allis, C. D. (1996) *Cell* 84, 843–851.
4. Felsenfeld, G. (1996) *Cell* 86, 13–19.
5. Kuo, M.-H., Zhou, J., Jambeck, P., Churchill, M. E. A., and Allis, C. D. (1998) *Genes Dev.* 12, 627–639.
6. Bouvet, P., Dimitrov, S., and Wolffe, A. P. (1994) *Genes Dev.* 8, 1147–1159.
7. Shen, X., and Gorovsky, M. A. (1996) *Cell* 86, 475–483.
8. Steinbach, O. C., Wolffe, A. P., and Rupp, R. (1997) *Nature* 389, 395–399.
9. Arents, G., Burlingame, R. W., Wang, B. W., Love, W. E., and Moudrianakis, E. N. (1991) *Proc. Natl. Acad. Sci. U.S.A.* 88, 10148–10152.
10. Arents, G., and Moudrianakis, E. N. (1993) *Proc. Natl. Acad. Sci. U.S.A.* 90, 10489–10493.
11. Arents, G., and Moudrianakis, E. N. (1995) *Proc. Natl. Acad. Sci. U.S.A.* 92, 11170–11174.
12. Luger, K., Mader, A. W., Richmond, R. K., Sargent, D. F., and Richmond, T. J. (1997) *Nature* 389, 251–260.
13. Pruss, D., Bartholomew, B., Persinger, J., Hayes, J., Arents, G., Moudrianakis, E. N., and Wolffe, A. P. (1996) *Science* 274, 614–617.
14. Hayes, J. J. (1996) *Biochemistry* 35, 11931–11937.
15. Crane-Robinson, C. (1997) *Trends Biochem. Sci.* 22, 75–77.
16. Lee, K. M., and Hayes, J. J. (1997) *Proc. Natl. Acad. Sci. U.S.A.* 94, 8959–8964.
17. Levina, E. S., Bavykin, S. G., Shick, V. V., and Mirzabekov, A. D. (1981) *Anal. Biochem.* 110, 93–101.
18. Mirzabekov, A. D., Shick, V. V., Belyavsky, A. V., and Bavykin, S. G. (1978) *Proc. Natl. Acad. Sci. U.S.A.* 75, 4184–4188.
19. Mirzabekov, A. D., and Rich, A. (1979) *Proc. Natl. Acad. Sci. U.S.A.* 76, 1118–1121.
20. Shick, V. V., Belyavsky, A. V., Bavykin, S. G., and Mirzabekov, A. D. (1980) *J. Mol. Biol.* 139, 491–517.
21. Belyavsky, A. V., Bavykin, S. G., Gogvadze, E. G., and Mirzabekov, A. D. (1980) *J. Mol. Biol.* 139, 519–536.
22. Bavykin, S. G., Usachenko, S. I., Zalsensky, A. O., and Mirzabekov, A. D. (1990) *J. Mol. Biol.* 212, 495–511.
23. Bavykin, S. G., Usachenko, S. I., Lishanskaya, A. I., Shick, V. V., Belyavsky, A. V., Undritsov, I. M., Stokov, A. A., Zalsenskaya, I. A., and Mirzabekov, A. D. (1985) *Nucleic Acids Res.* 13, 3439–3459.
24. Usachenko, S. I., Bavykin, S. G., Gavin, I. M., and Bradbury, E. M. (1994) *Proc. Natl. Acad. Sci. U.S.A.* 91, 6845–6849.
25. Usachenko, S. I., Gavin, I. M., and Bavykin, S. G. (1996) *J. Biol. Chem.* 271, 3831–3836.
26. Pruss, D., Hayes, J. J., and Wolffe, A. P. (1995) *BioEssays* 17, 161–170.
27. Hayes, J. J., Tullius, T. D., and Wolffe, A. P. (1990) *Proc. Natl. Acad. Sci. U.S.A.* 87, 7405–7409.
28. Hayes, J. J., Pruss, D., and Wolffe, A. P. (1994) *Proc. Natl. Acad. Sci. U.S.A.* 91, 7817–7821.
29. Simpson, R. T. (1978) *Biochemistry* 17, 5524–5521.
30. Allan, J., Hartman, P. G., Crane-Robinson, C., and Aviles, F. X. (1980) *Nature* 288, 675–679.
31. Staynov, D. Z., and Crane-Robinson, C. (1988) *EMBO J.* 7, 3685–3691.
32. Hayes, J. J., and Wolffe, A. P. (1993) *Proc. Natl. Acad. Sci. U.S.A.* 90, 6415–6419.
33. Wong, J., Shi, Y.-B., and Wolffe, A. P. (1995) *Genes Dev.* 9, 2696–2711.
34. Wong, J., Shi, Y.-B., and Wolffe, A. P. (1997) *EMBO J.* 16, 3158–3171.
35. Wong, J., Li, Q., Levi, B.-Z., Shi, Y.-B., and Wolffe, A. P. (1997) *EMBO J.* 16, 7130–7145.
36. Wong, J., Patterson, D., Imhof, A., Guschin, D., Shi, Y.-B., and Wolffe, A. P. (1998) *EMBO J.* 17, 520–534.
37. Tatchell, K., and van Holde, K. E. (1977) *Biochemistry* 16, 5295–5303.
38. Hayes, J. J., and Wolffe, A. P. (1992) *Proc. Natl. Acad. Sci. U.S.A.* 89, 1229–1233.
39. Mirzabekov, A. D., Bavykin, S. G., Belyavsky, A. V., Karpov, V. L., Preobrazhenskaya, O. V., Schick, V. V., and Ebralidze, K. K. (1989) *Methods Enzymol.* 170, 386–408.
40. Bashkin, J., Hayes, J. J., Tullius, T. D., and Wolffe, A. P. (1993) *Biochemistry* 32, 1895–1898.
41. Meersseman, G., Pennings, S., and Bradbury, E. M. (1992) *EMBO J.* 11, 2951–2959.
42. Ura, K., Hayes, J. J., and Wolffe, A. P. (1995) *EMBO J.* 14, 3752–3765.
43. Richmond, T. J., Finch, J. T., Rushton, B., Rhodes, D., and Klug, A. (1984) *Nature* 311, 532–537.
44. Ebralidze, K. K., Grachev, S. A., and Mirzabekov, A. D. (1988) *Nature* 331, 365–367.
45. Lindsey, G. G., Orgeig, S., Thompson, P., Davies, N., and Maeder, D. L. (1991) *J. Mol. Biol.* 218, 805–813.
46. Gushchin, D. Y., Ebralidze, K. K., and Mirzabekov, A. D. (1991) *Mol. Biol.* 25, 1400–1411.
47. Pruss, D., and Bavykin, S. G. (1997) *Methods* 12, 36–47.
48. Pehrson, J. R. (1989) *Proc. Natl. Acad. Sci. U.S.A.* 86, 9149–9153.
49. Goytisolo, F. A., Gerchman, S. E., Yu, X., Rees, C., Graziano, V., Ramakrishnan, V., and Thomas, J. O. (1996) *EMBO J.* 15, 3421–3429.
50. Lennard, A. C., and Thomas, J. O. (1985) *EMBO J.* 4, 3455–3462.

51. Cirillo, L. A., McPherson, C. E., Bossard, P., Stevens, K., Cherian, S., Shim, E. Y., Clark, K. L., Burley, S. K., and Zaret, K. S. (1998) *EMBO J.* 17, 244–254.
52. Hayes, J. J., Kaplan, R., Ura, K., Pruss, D., and Wolffe, A. P. (1996) *J. Biol. Chem.* 271, 25817–25822.
53. An, W., Leuba, S. H., van Holde, K. E., and Zlatanova, J. (1998) *Proc. Natl. Acad. Sci. U.S.A.* 95, 3396–3401.
54. Sera, T., and Wolffe, A. P. (1998) *Mol. Cell. Biol.* (in press).
55. Peterson, R. C., Doering, J. L., and Brown, D. D. (1980) *Cell* 20, 131–141.
56. Simpson, R. T., and Stafford, D. W. (1983) *Proc. Natl. Acad. Sci. U.S.A.* 80, 51–55.

BI9805846